2023 12th International Conference on Renewable Energy Research and Applications (ICRERA) | 979-8-3503-3793-8/23/$31.00 ©2023 IEEE | DOI: 10.1109/ICRERA59003.2023.10269376

Model Predictive Control of Dual Three-Phase Four-Leg Multilevel Inverter Supplying Photovoltaic Energy to Low-Voltage Unbalanced Grids

Joaquim Monteiro
ISEL – Polytechnic Institute of Lisboa, Lisboa, Portugal
INESC-ID Lisboa, Portugal
joaquim.monteiro@isel.pt

V. Fernão Pires
Sustain.RD, ESTSetúbal, Instituto Politécnico Setúbal, Setubal Portugal
INESC-ID Lisboa, Portugal
vitor.pires@estsetubal.ips.pt

J. Fernando Silva
DEEC, IST, Universidade de Lisboa, Lisboa, Portugal
INESC-ID Lisboa, Portugal
fernando.alves@tecnico.ulisboa.pt

Sónia Pinto
DEEC, IST, Universidade de Lisboa, Lisboa, Portugal
INESC-ID Lisboa, Portugal
soniafp@tecnico.ulisboa.pt

***Abstract* - In this paper, a new control system is proposed for a grid-connected photovoltaic (PV) generation system based on a dual three-phase four leg multilevel inverter. This power converter topology, built using two four-leg two-level three-phase inverters, connects two PV arrays in the DC side to three open-end-windings of a three-phase transformer on the AC side. This arrangement is controlled to inject the PV generated power into the low voltage (LV) grid allowing support for unbalanced loads. The proposed control system is based in the model predictive control (MPC). It allows the control of the injected grid currents in balanced/unbalanced conditions while ensuring the balance of the capacitor DC voltages. Several simulation tests are made to validate the effectiveness of the control strategy applied to the proposed PV generation system.**

Keywords— Dual inverter, multilevel inverter, four-leg two-level inverter, photovoltaic system (PV); model predictive control (MPC)

I. INTRODUCTION

In recent years, there has been significant advancement in renewable energy sources, as well as the systems required for their proper operation. Most distributed renewable energy sources need power electronic converters to interface the generation technology to the AC grid [1-3]. In this context, photovoltaic (PV) systems are well suited to distributed generation in low voltage (LV) grids, where the inverter is a critical piece of equipment [4-7].

In addition to generating renewable energy, PV systems can provide ancillary services to LV electrical distribution grids to conserve power quality. Overvoltages/undervoltages, reactive power injection, current harmonics and voltage unbalances are power quality issues that affect LV networks [7]. Several studies [7, 8] proposed using PV generators to provide ancillary services in power quality enhancement, an interesting solution to mitigate voltage unbalances due to unbalanced loads. Indeed, the uneven distribution of single-phase loads, as well as non-linear loads generating 3rd order harmonics or unpredictable phenomena in grids, will generate currents in the neutral wire leading to zero-sequence current components [9].

Several power quality issues can be mitigated using the capabilities of PV generators, which can also provide ancillary services, such as reactive power control and harmonics in LV grids [10-12]. Nevertheless, several alternatives to PV approaches have been proposed to support the grid in mitigating unbalanced load effects on the LV grids [13, 14]. In fact, some researchers provided grid-connected PV generators with the capability of inject unbalanced currents in the grid [15, 16]. PV generators typically employ two-level three-phase voltage source inverters (VSIs) with a four-leg topology [16, 17]. However, for power quality applications PV grid-connection using multilevel VSIs is a strong alternative to the use of two-level VSIs. Therefore, several multilevel topologies for PV grid connection have been proposed. Among them, conventional multilevel topologies like the neutral point clamped (NPC), the flying capacitor and the cascaded H-bridge converter structure [18–22], have been adopted and extensively studied. Despite the fact that multilevel inverters have a number of advantages over their two-level equivalents, few works have been proposed using multilevel inverters to support unbalanced LV networks. One of these more recent works that suggested multilevel inverters was published in [23]. This proposal, which contains two traditional four-leg VSIs, is based on a modular industrial interesting solution. However, [23] is focused on the topology and do not thoroughly considered the control system. While the majority of the works use traditional modulation methods like sinusoidal PWM [22], several non-linear control methods can be applied to power electronic converters, like model predictive control (MPC), which is widely, used producing recognized good results [24-28]. Indeed, MPC is characterized by fast dynamic response, ease of design, and capability to include non-linearity and system constraints [29].

This paper presents a new control system for a dual inverter PV five-level system based on a modular structure, each module using a four-leg three-phase two-level inverter. The control system is designed with the purpose to also support unbalanced grids (LV with neutral connection). In this way, when the PV power is enough upstream of this PV generator the power flow will be balanced. The model predictive controller approach is used in the proposed new controller. The predictive controller was designed to take into account the various variables that must be controlled in the grid-connected dual PV generator to balance the DC side capacitor voltages. Several simulation tests in steady and transient states will be presented and discussed to confirm the performance and characteristics of the implemented control system.

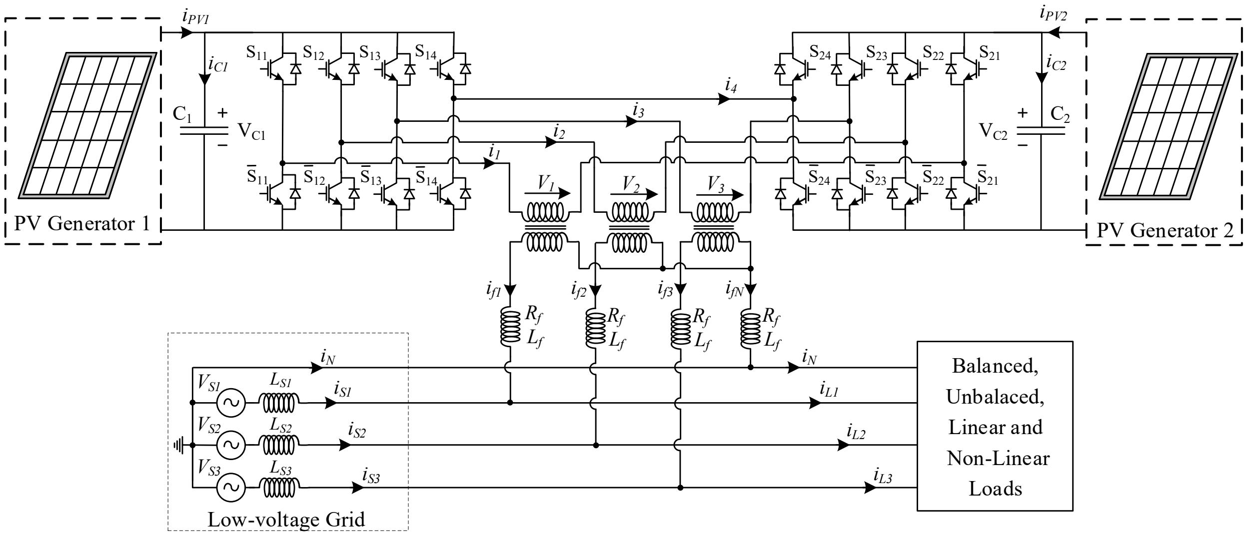

Fig. 1. Multilevel topology for grid-connected PV systems based on four-leg inverters and OeW transformer.

II. FOUR-LEG TWO-LEVEL INVERTER TOPOLOGY

The dual inverter topology is one of the most recent four wire multilevel topologies that can be used in grid-connected PV generation systems. This multilevel structure is built around two four-leg two-level VSIs connected to the three open end windings (OeW) of a three-phase transformer. The two DC buses are fed from two PV arrays, as shown in Fig. 1.

Applying the Kirchhoff laws and the state of the switches to the dual three-phase four-leg multilevel inverters of the power circuit, presented in Fig. 1, the OeW transformer primary AC voltages V_1, V_2, V_3 can be obtained. In fact, considering the power switches as ideal and represented by a binary variable γ_{ji} (where i = 1:4 represents the inverter leg and j = 1,2 the inverter number), the AC voltages V_1, V_2, V_3 are given through the difference between the AC voltages of each inverter:

$$\begin{bmatrix} V_1 \\ V_2 \\ V_3 \end{bmatrix} = V_{C1}\begin{bmatrix} 1 & 0 & 0 & -1 \\ 0 & 1 & 0 & -1 \\ 0 & 0 & 1 & -1 \end{bmatrix}\begin{bmatrix} \gamma_{11} \\ \gamma_{12} \\ \gamma_{13} \\ \gamma_{14} \end{bmatrix} - V_{C2}\begin{bmatrix} 1 & 0 & 0 & -1 \\ 0 & 1 & 0 & -1 \\ 0 & 0 & 1 & -1 \end{bmatrix}\begin{bmatrix} \gamma_{21} \\ \gamma_{22} \\ \gamma_{23} \\ \gamma_{24} \end{bmatrix} \quad (1)$$

where V_{Cj} corresponds to the DC voltages of each inverter and the binary variable, γ_{ji}, is directly related to the state of switch S_{ji} ($\gamma_{ji} = 1$ if the switch is ON, while $\gamma_{ji} = 0$ if it is OFF).

By applying the Clarke-Concordia transformation to the five-level AC voltages in the expression (1), 256 different output voltage space vectors can be devised, although only 65 of them are distinct voltage vectors [21].

Analyzing the power circuit given in Fig. 1, the following state equations for the DC capacitor voltages can be obtained:

$$\frac{d}{dt}\begin{bmatrix} v_{C1} \\ v_{C2} \end{bmatrix} = \begin{bmatrix} \frac{1}{C_1} & 0 \\ 0 & \frac{1}{C_2} \end{bmatrix}\begin{bmatrix} i_{PV1} \\ i_{PV2} \end{bmatrix} - \begin{bmatrix} \frac{1}{C_1} & 0 \\ 0 & \frac{1}{C_2} \end{bmatrix}\begin{bmatrix} i_{C1} \\ i_{C2} \end{bmatrix} \quad (2)$$

where currents i_{C1} and i_{C2} are given by (3). Currents i_{PV1} and i_{PV2} are the independent currents of each PV generator and C_1 and C_2 are the DC link capacitances of each inverter.

$$\begin{bmatrix} i_{C1} \\ i_{C2} \end{bmatrix} = \begin{bmatrix} \gamma_{11} & \gamma_{12} & \gamma_{13} & \gamma_{14} \\ -\gamma_{21} & -\gamma_{22} & -\gamma_{23} & -\gamma_{24} \end{bmatrix}\begin{bmatrix} i_1 \\ i_2 \\ i_3 \\ i_4 \end{bmatrix} \quad (3)$$

Using a similar analysis, the following state space equations for the AC secondary currents in $\alpha\beta 0$ coordinates can be obtained.

$$\frac{d}{dt}\begin{bmatrix} i_\alpha \\ i_\beta \\ i_o \end{bmatrix} = \begin{bmatrix} -\frac{R_f}{L_f} & 0 & 0 \\ 0 & -\frac{R_f}{L_f} & 0 \\ 0 & 0 & -\frac{R_f}{L_f} \end{bmatrix}\begin{bmatrix} i_\alpha \\ i_\beta \\ i_o \end{bmatrix} + \begin{bmatrix} -v_{C1} & 0 & 0 \\ 0 & -v_{C1} & 0 \\ 0 & 0 & -v_{C1} \end{bmatrix}\begin{bmatrix} \gamma_{1\alpha} \\ \gamma_{1\beta} \\ \gamma_{1o} \end{bmatrix} + \begin{bmatrix} -v_{C2} & 0 & 0 \\ 0 & -v_{C2} & 0 \\ 0 & 0 & -v_{C2} \end{bmatrix}\begin{bmatrix} \gamma_{2\alpha} \\ \gamma_{2\beta} \\ \gamma_{2o} \end{bmatrix} + \begin{bmatrix} -\frac{1}{L_f} & 0 & 0 \\ 0 & -\frac{1}{L_f} & 0 \\ 0 & 0 & -\frac{1}{L_f} \end{bmatrix}\begin{bmatrix} V_{s\alpha} \\ V_{s\beta} \\ V_{so} \end{bmatrix} \quad (4)$$

where R_f and L_f are the resistance and inductance, respectively, of the interface inductor to each phase and neutral wires of the LV grid.

These dynamic model equations (4) of the dual three-phase four-leg multilevel converter, will be used in the design of the power systems controllers.

III. Model Predictve Control Method

The control method applied to the dual three-phase four-leg multilevel inverter is based on MPC principles [23, 25, 27], according to the scheme shown in Fig. 2.

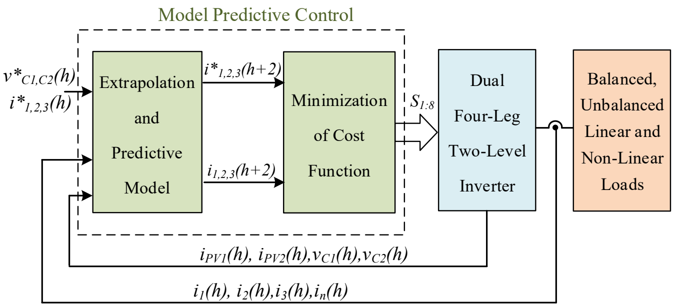

Fig. 2. Model predictive control scheme to control the multilevel inverter.

The proposed control method uses the power system dynamic model (4), developed in the last section, to calculate the future behavior of the system. In this control method, the actual values of the AC injected grid currents, the capacitors voltages are measured in the h instant. Based on these values, the AC currents injected into the grid, and the voltages of the capacitors can be predicted for the h+1 instant. The selection of the optimal voltage vector is made by minimizing a defined cost functional, therefore ensuring the minimum value for the function of the errors between references and their predicted values. The whole process is repeated for each sampling instant h, considering the acquired data in the previous sampling instant h-1. The time taken by the control algorithm calculations is compensated by introducing delay compensation techniques.

Consequently, based on this principle and the control scheme presented in Fig. 2, the AC currents injected into the grid, in αβo coordinates, i_k (k=α, β, o) at the t_{h+1} instant, can be predicted according to expression (5):

$$i_k(h+1)=\left(1-\frac{R_f}{L_f}T_S\right)i_k(h)+\frac{T_S}{L_f}\left(v_k(h)-V_{Sk}(h)\right) \qquad (5)$$

where i_k ($h+1$) and i_k (h) are the predicted value of current for sampling interval time instant $t(h+1)$ and the current measured, respectively, T_S is the sampling time, V_{Sk} (h) and v_k (h) are respectively, the source and the converter voltages.

The discrete time equation for the capacitors C_j (j = 1, 2) voltages, using MPC strategy, is obtained in (6):

$$v_{Cj}(h+1)=v_{Cj}(h)+\frac{1}{C_j}i_{Cj}(h)T_S \qquad (6)$$

where the current $i_{Cj}(h)$ depend on the switching states of the dual three-phase four-leg multilevel converter and the value of the currents, in accordance to (7) and (8):

$$i_{C1}(h)=i_{PV1}(h)-S_{11}i_1-S_{12}i_2-S_{13}i_3-S_{14}i_4 \qquad (7)$$

$$i_{C2}(h)=i_{PV2}(h)+S_{21}i_1+S_{22}i_2+S_{23}i_3+S_{24}i_4 \qquad (8)$$

With the aim to compensate for the computational time spent on the evaluation control algorithm, delay compensation techniques have been established. The compensation method consists of using for the predictive control method the future current at $t(h+2)$ instant, in (9).

$$i_k(h+2)=\left(1-\frac{R_f}{L_f}T_S\right)i_k(h+1)+\frac{T_S}{L_f}\left(v_k(h+1)-V_{Sk}(h+1)\right) \qquad (9)$$

Applying the same reasoning, for the delay compensation of the DC capacitors voltage, by time-shifting the model (6) one step forward as follows:

$$v_{Cj}(h+2)=v_{Cj}(h+1)+\frac{1}{C_j}i_{Cj}(h+1)T_S \qquad (10)$$

The MPC cost function is comprised of two weighted cost terms, for injected grid currents and for the capacitors voltage imbalance. For the currents, the cost function is given by:

$$\begin{aligned} g_i = &\left|i_\alpha^*(h+2)-i_\alpha(h+2)\right|\rho_{i\alpha}+\left|i_\beta^*(h+2)-i_\beta(h+2)\right|\rho_{i\beta} \\ &+\left|i_o^*(h+2)-i_o(h+2)\right|\rho_{io} \end{aligned} \qquad (11)$$

where $i_\alpha^*(h+2)$, $i_\beta^*(h+2)$, $i_o^*(h+2)$ are respectively, the α, β and zero parts, of the injected grid currents references and $i_\alpha(h+2)$, $i_\beta(h+2)$, $i_o(h+2)$ are respectively, the α, β and zero parts, of the injected grid currents predicted. $\rho_{i\alpha},\rho_{i\beta},\rho_{io}$ are the weighting factors, for real, imaginary and homopolar parts of the current.

The DC capacitor voltages must remain tightly regulated to minimize unbalances on the grid AC voltages, as the transformer primary voltages are related to the DC voltages. Therefore, the cost function of the DC capacitors voltages imbalance is defined as:

$$g_{vdc}=\left|v_{C1}(h+2)-v_{C2}(h+2)\right|\rho_{vdc} \qquad (12)$$

where $v_{C1}(h+2), v_{C2}(h+2)$ are the predicted voltages of the C_1 and C_2 capacitors, and ρ_{vdc} the respective weighting factor.

Finally, the proposed cost function of the model power system will be given by adding the previous cost functionals.

$$g=g_i+g_{vdc} \qquad (13)$$

In the next section, the predictive control strategy will be implemented for Simulation in the MATLAB Software, containing the previous expressions.

IV. Simulation Results

To verify the performance of the proposed topology, for grid-connected PV systems, with the proposed control system, several simulations results were made. These simulation results were performed using MATLAB/Simulink and SimPowerSystems library. The system is connecting to a grid with 230/400 V_{rms} 50 Hz, through transformers with a turns-ratio of 1:1. All the other parameters used in numerical tests are presented in the Table I.

TABLE I. Parameters of the System

Input DC voltage	480 V
Capacitors C1 and C2	5 mF
Resistor per phase (R_f)	5 Ω
Inductor per phase (L_f)	5 mH

The simulation conditions employed to investigate the MPC, applied to the grid-connected photovoltaic generation system proposed, allow to test balanced and unbalanced currents. The references are generated in accordance with [11]. Several tests were made under different system requirements. Fig. 3 presents the voltage waveform applied to the primary winding of the transformer, in the phase 1. This result illustrates the five voltage levels, where the maximum value is twice the DC voltage of each converter.

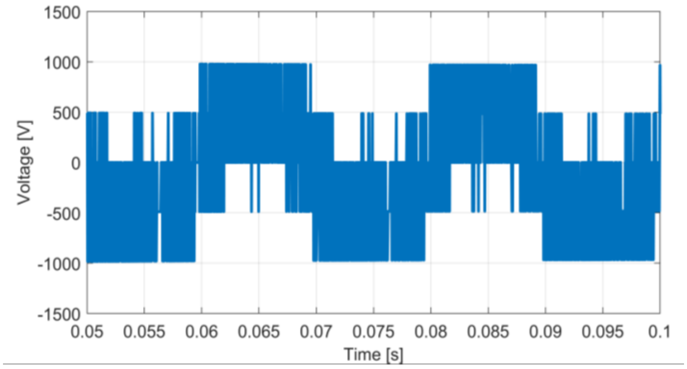

Fig. 3. Waveform of the voltage V_1 applied to the primary winding of the transformer.

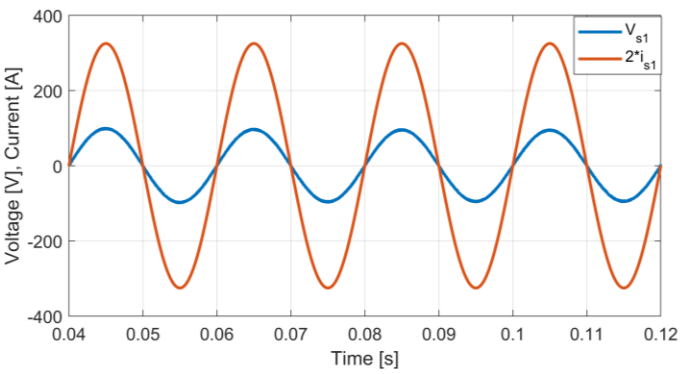

Fig. 4. Waveform of the grid voltage and AC current of phase 1 in steady-state condition.

The results presented in Fig. 4 exhibit the current and the grid voltage at the same phase, for balanced currents. These results show that the current is in phase with the voltage, guaranteeing a near unity power factor.

In order to verify the behavior of the power system in dynamic conditions, a test in which the currents are initially balanced and suddenly change to unbalanced. The transient test, considering that the system is initially balanced and suddenly undergoes to unbalanced operation was performed. Fig 5 shows the result of this test, where it is possible confirm that up to the instant 0.15s the three-phase currents are balanced (neutral current is zero), and after this instant the currents immediately change to unbalanced. This result confirms the fast response of the proposed control method.

Based on the previous transient conditions, in Fig. 6 it is also possible to verify that the current and the grid voltage in the transformer primary are in phase, even for a transient regime. Fig. 7 shows the DC voltage at the terminals of capacitors, C_1 and C_2, for the same transient state, where it is seen that the DC capacitors voltages are close to the same value and stable even after the change of the balanced to unbalanced operation.

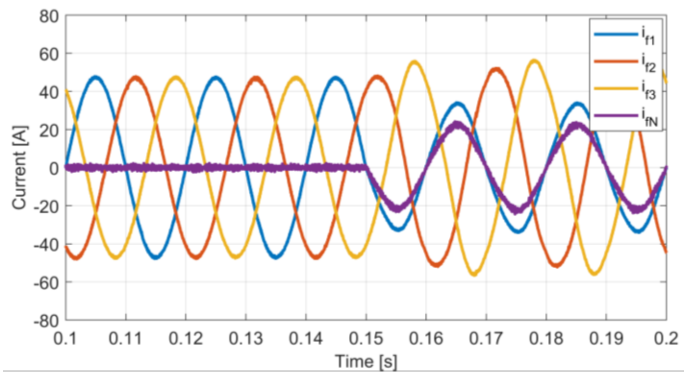

Fig. 5. Simulation results of the injected currents into the grid under transient conditions (balanced to unbalanced).

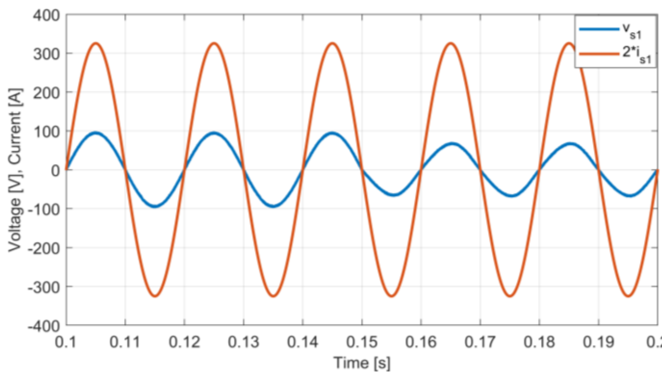

Fig. 6. Waveform of the grid voltage and AC current of phase 1 in transient conditions (balanced to unbalanced).

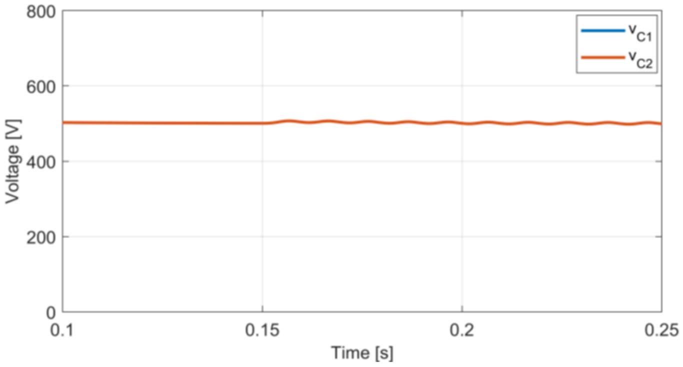

Fig. 7. Simulation results of capacitors C_1 and C_2 voltage, under transient conditions (balanced to unbalanced).

Next figures include detailed simulation results, showing another test for different dynamic conditions. To show the dynamic behaviour of the proposed MPC controller of the dual three-phase four-leg multilevel inverter. In this transient test the system is unbalanced and suddenly the power provided by the PV panels decreases. Fig 8 shows the AC currents injected in the grid at unbalanced conditions and in which at instant t=0.3s the power generated by the PV panels decreases suddenly. This result illustrates that the injected AC currents into the grid follow the respective power variation, presenting low distortion.

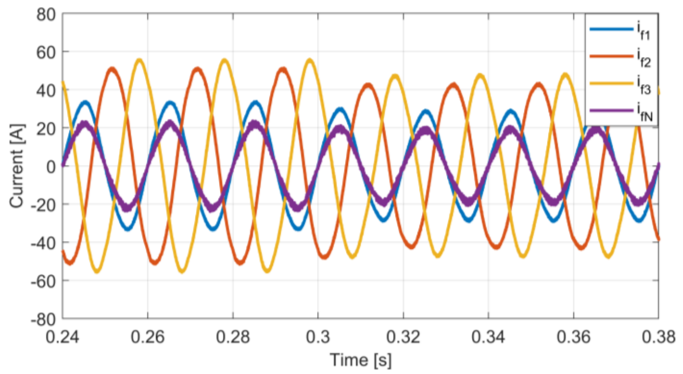

Fig. 8. Simulation results of the injected currents into the grid under transient conditions when the generated power decreases at t=0.3s (unbalanced to unbalanced).

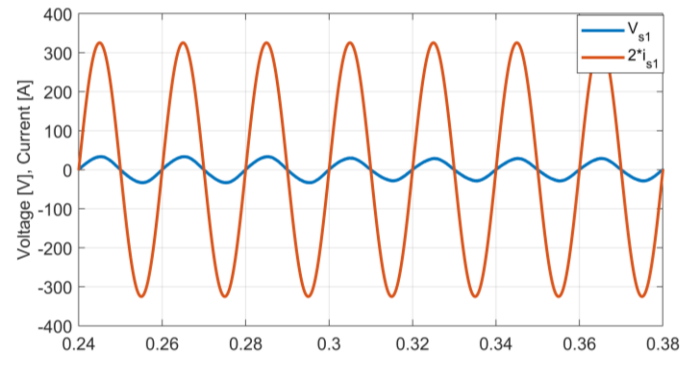

Fig. 9. Waveform of the grid voltage and AC current of phase 1 under transient conditions when the generated power decreases at t=0.3s (unbalanced to unbalanced).

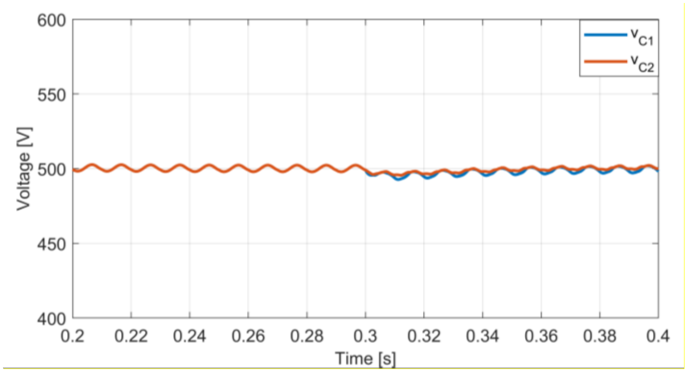

Fig. 10. Simulation results of capacitors C_1 and C_2 voltage, under transient conditions when the generated power decreases at t=0.3s (unbalanced to unbalanced).

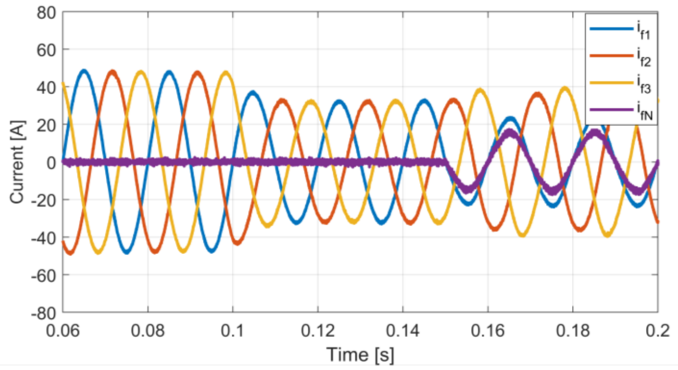

Fig. 11. Simulation results of the injected currents into the grid under transient conditions when the generated power decreases at t=0.1s and then at t=0.15s the system suddenly change from balanced to unbalanced.

From the analysis of the Fig. 9, it is concluded that the current is in phase with grid voltage in the primary winding maintaining the same phase in transient conditions, even when there is a decrease in generated power. Fig. 10 shows the capacitors voltages, being possible to see that they remain stable and close to the reference values. Fig 11 shows the AC currents injected in the grid when the system is balanced and suddenly the power generated decrease at instant t=0.1s and then at instant t=0.15s started to support the grid in an unbalanced way. These results confirm the fast response of the proposed control method.

Simulation results of the MPC scheme for the grid-connected PV systems, has shown that the response of the controllers is in accordance with the proposed approach.

V. Conclusions

This paper has presented the predictive control applied to a modular structure with two classical three-phase four-leg two-level inverters coupled to OeW transformer to obtain a five-level converter. The proposed controller not only allowed to control the inject currents into the grid, with balanced/unbalanced loads, but also ensures the balance and regulation of the capacitors DC voltage. In this predictive controller, a cost function of the errors between the reference and the predicted control variables was evaluated, resulting in the weighted addition of two partial cost functions. Simulation results show that using the proposed control system, the balancing of the capacitors voltage was achieved and the injected grid currents, either in balanced/unbalanced situation, were controlled, showing a fast and robust dynamic response. The obtained results, in steady-state and in transient conditions, confirm the expected performance of the control method used in the dual three-phase four-leg multilevel inverter topology.

ACKNOWLEDGMENT

This work was supported by national funds through FCT – Fundação para a Ciência e a Tecnologia, under project UIDB/50021/2020.

REFERENCES

[1] F. Blaabjerg, Y. Yang, K. Ma, X. Wang, “Power electronics - the key technology for renewable energy system integration” Int. Conf. Renewable Energy Research Appl., pp. 1618-1626, Nov. 2015

[2] P. Roy, J. He, T. Zhao and Y. V. Singh, "Recent Advances of Wind-Solar Hybrid Renewable Energy Systems for Power Generation: A Review," in IEEE Open Journal of the Industrial Electronics Society, vol. 3, pp. 81-104, January 2022.

[3] A. Oymak, M. R. Tur, “A Short Review on the Optimization Methods Using for Distributed Generation Planning”, International Journal of Smart Grid (ijSmartGrid) vol. 6, no. 3, pp. 54-64, September 2022.

[4] M. E. T. Souza Junior and L. C. G. Freitas, “Power Electronics for Modern Sustainable Power Systems: Distributed Generation, Microgrids and Smart Grids—A Review,” Sustainability, vol. 14, no. 6, p. 3597, March 2022.

[5] Ali Khan, M.Y., Liu, H.; Yang, Z.; Yuan, X. A comprehensive review on grid connected photovoltaic inverters, their modulation techniques, and control strategies. Energies, vol. 13, p. 4185, 2020.

[6] V. F. Pires, J. Monteiro and J. F. Silva, "A Grid-Connected PV Multilevel Cascaded Inverter System Based on Single and Three-Phase Two-Level Inverters," 8th International Conference on Renewable Energy Research and Applications (ICRERA), pp. 118-123, 2019

[7] F. Alsokhiry and K. L. Lo, "Provision of reactive power support ancillary services from distributed generation based on renewable energy," International Conference on Renewable Energy Research and Applications (ICRERA), pp. 1018-1023, 2013.

[8] R. Panigrahi, S. K. Mishra, S. C. Srivastava, A. K. Srivastava and N. N. Schulz, "Grid Integration of Small-Scale Photovoltaic Systems in Secondary Distribution Network—A Review," IEEE Transactions on Industry Applications, vol. 56, no. 3, pp. 3178-3195, May-June 2020

[9] J. J. M. Desmet, I. Sweertvaegher, G. Vanalme, K. Stockman and R. J. M. Belmans, "Analysis of the neutral conductor current in a three-phase supplied network with nonlinear single-phase loads," in IEEE Transactions on Industry Applications, vol. 39, no. 3, pp. 587-593, May-June 2003.

[10] R. Hu, W. Wang, X. Wu, Z. Chen, L. Jing, W. Ma, G. Zeng, "Coordinated active and reactive power control for distribution networks with high penetrations of photovoltaic systems," Solar Energy, vol. 231, no. 2, pp. 809-827, January 2022.

[11] G. D. Marques, V. F. Pires, M. Malinowski and M. Kazmierkowski, “An Improved Synchronous Reference Frame Method for Active Filters,” EUROCON - The International Conference on "Computer as a Tool", pp. 2564-2569, September 2007, doi: 10.1109/EURCON.2007.4400408.

[12] R. Aljarrah, M. S. Ayaz, Q. Salem, M. Al-Omary, I. Abuishmais, W. Al-Rousan, “Application of Passive Harmonic Filters in Power Distribution System with High Share of PV Systems and Non-Linear Loads”, International Journal of Renewable Energy Research, vol. 13, no. 1, pp. 401-411, March 2023.

[13] V. F. Pires, O. Husev, D. Vinnikov and J. F. Martins, "A control strategy for a grid-connected PV system with unbalanced loads compensation," 9th International Conference on Compatibility and Power Electronics (CPE), pp. 154-159, June 2015.

[14] E. M. Ahmed, M. Aly, A. Elmelegi, A. G. Alharbi, and Z. M. Ali, “Multifunctional Distributed MPPT Controller for 3P4W Grid-Connected PV Systems in Distribution Network with Unbalanced Loads,” Energies, vol. 12, no. 24, p. 4799, December 2019.

[15] F. -J. Lin, K. -H. Tan, Y. -K. Lai and W. -C. Luo, "Intelligent PV Power System With Unbalanced Current Compensation Using CFNN-AMF," in IEEE Transactions on Power Electronics, vol. 34, no. 9, pp. 8588-8598, Sept. 2019.

[16] F. H. M. Rafi, M. J. Hossain and J. Lu, "Improved Neutral Current Compensation With a Four-Leg PV Smart VSI in a LV Residential Network," in IEEE Transactions on Power Delivery, vol. 32, no. 5, pp. 2291-2302, October 2017.

[17] D. V. Bozalakov, M. J. Mnati, J. Laveyne, A. V. d. Bossche and L. Vandevelde, "Voltage Unbalance and Overvoltage Mitigation by Using the Three-phase Damping Control Strategy in Battery Storage Applications," 7th International Conference on Renewable Energy Research and Applications (ICRERA), 2018.

[18] I. Colak, E. Kabalci, R. Bayindir, “Review of multilevel voltage source inverter topologies and control schemes”, Energy conversion and management, vol. 52, pp. 1114–1128, February 2011.

[19] V. F. Pires, A. Cordeiro, D. Foito and J. F. Silva, "A Multilevel Converter Topology for a STATCOM System Based on Four-Leg Two-Level Inverters and Cascaded Scott Transformers," IEEE Transactions on Power Delivery, vol. 37, no. 3, pp. 1391-1402, June 2022.

[20] F. Muhammad, H. Rasheed, “Power Loss Distribution And Characterization Of Modular Multilevel Converter For Smart Grid Applications”, International Journal of Renewable Energy Research, vol. 12, no. 3, pp. 1540-1551, September 2022.

[21] M. Bouzidi, S. Barkat, A. Krama and H. Abu-Rub, "Simplified Predictive Direct Power Control of Three-Phase Three-Level Four-Leg Grid Connected NPC Converter," in IEEE Open Journal of the Industrial Electronics Society, vol. 3, pp. 448-459, 2022.

[22] V. F. Pires, A. Cordeiro, D. Foito, A. J. Pires, C. Hao, J. F. Martins, R. Castro, “Compensation of Unbalanced Low-Voltage Grids Using a Photovoltaic Generation System with a Dual Four-Leg, Two-Level Inverter,” Electronics, Vol. 11, Issue 3, pp. 1-25, February 2022.

[23] V. F. Pires, A. Cordeiro, D. Foito, A. J. Pires, H. Chen, J. F. Martins, R. Castro, "A Cascaded Dual Four-Leg Inverter for Photovoltaic Systems With Capability to Compensate Unbalanced Distribution Networks," in IEEE Journal of Emerging and Selected Topics in Industrial Electronics, vol. 4, no. 3, pp. 960-968, July 2023.

[24] M. Rivera, V. Yaramasu, A. Llor, J. Rodriguez, B. Wu, M. Fadel, “Digital predictive current control of a three-phase four-leg inverter,” IEEE Transactions on Industrial Electronics, vol. 60, no. 11, pp. 4903–4912, Nov. 2013.

[25] J. Monteiro, V. F. Pires, J. F. Silva and S. Pinto, "Mutilevel Bipolar Back-to-Back HVDC Transmission System Based on the Dual Inverter Converter Structure with Model Predictive Control," Annual Conference of the IEEE Industrial Electronics Society, pp. 1-6, October 2022.

[26] J. D. Barros, JF Silva, Optimal predictive control of three-phase NPC multilevel converter for power quality applications IEEE Transactions on Industrial Electronics, vol.55 no. 10, pp 3670-3681, 2008.

[27] F. Selim, T. F. Megahed, M. Aly, M. Shoyama and S. M. Abdelkader, "Model Predictive Control Based Improved Techno-Economic Control Strategy for Photovoltaic-Battery Microgrids," 11th International Conference on Renewable Energy Research and Application (ICRERA), pp. 230-235, September 2022.

[28] J. D. Barros, J. F. Silva, É. Jesus, “Fast-Predictive Optimal Control of NPC Multilevel Converters,” IEEE Trans. Ind. Electron., vol. 60, no. 2, pp. 619-627, February 2013.

[29] S. Vazquez, J. Leon, L. Franquelo, J. Rodriguez, H. Young, A. Marquez, P. Zanchetta, “Model Predictive Control: A Review of Its Applications in Power Electronics,” IEEE Ind. Electron. Mag., vol. 8, no. 1, pp. 16-31, Mar. 2014.